

# A semi-implicit level set method for structural shape and topology optimization

Junzhao Luo<sup>a</sup>, Zhen Luo<sup>b</sup>, Liping Chen<sup>a</sup>, Liyong Tong<sup>b,\*</sup>, Michael Yu Wang<sup>c</sup>

<sup>a</sup> National Engineering Research Center for CAD, School of Mechanical Science and Engineering, Huazhong University of Science and Technology, Wuhan, Hubei 430074, PR China

<sup>b</sup> School of Aerospace, Mechanical and Mechatronic Engineering, The University of Sydney, NSW 2006, Australia

<sup>c</sup> Department of Mechanical and Automation Engineering, The Chinese University of Hong Kong, Shatin N.T., Hong Kong SAR, PR China

Received 27 September 2007; received in revised form 28 November 2007; accepted 3 February 2008

Available online 15 February 2008

## Abstract

This paper proposes a new level set method for structural shape and topology optimization using a semi-implicit scheme. Structural boundary is represented implicitly as the zero level set of a higher-dimensional scalar function and an appropriate time-marching scheme is included to enable the discrete level set processing. In the present study, the Hamilton–Jacobi partial differential equation (PDE) is solved numerically using a semi-implicit additive operator splitting (AOS) scheme rather than explicit schemes in conventional level set methods. The main feature of the present method is it does not suffer from any time step size restriction, as all terms relevant to stability are discretized in an implicit manner. The semi-implicit scheme with additive operator splitting treats all coordinate axes equally in arbitrary dimensions with good rotational invariance. Hence, the present scheme for the level set equations is stable for any practical time steps and numerically easy to implement with high efficiency. Resultantly, it allows enhanced relaxation on the time step size originally limited by the Courant–Friedrichs–Lewy (CFL) condition of the explicit schemes. The stability and computational efficiency can therefore be greatly improved in advancing the level set evolutions. Furthermore, the present method avoids additional cost to globally reinitialize the level set function for regularization purpose. It is noted that the periodically applied reinitializations are time-consuming procedures. In particular, the proposed method is capable of creating new holes freely inside the design domain via boundary incorporating, splitting and merging processes, which makes the final design independent of initial guess, and helps reduce the probability of converging to a local minimum. The availability of the present method is demonstrated with two widely studied examples in the framework of the structural stiffness designs.

© 2008 Elsevier Inc. All rights reserved.

**Keywords:** Shape optimization; Topology optimization; Level set methods; Semi-implicit schemes

\* Corresponding author. Tel.: +61 2 93516949; fax: +61 2 93514841.

E-mail addresses: [zluo@aeomech.usyd.edu.au](mailto:zluo@aeomech.usyd.edu.au) (Z. Luo), [ltong@aeomech.usyd.edu.au](mailto:ltong@aeomech.usyd.edu.au) (L. Tong).

## 1. Introduction

Several topology optimization methods have been developed in the past decades, such as the homogenization method [10], the solid isotropic microstructure with penalty (SIMP) method [11], the evolutionary structural optimization (ESO) method [70], the level set-based method [60,2] and so on. These methods have gained widespread popularity and are being applied to a wide range of engineering areas [1,12,22,46]. Both the homogenization method and the SIMP approach can be regarded as the material distribution approach, while the level set method is classified as a family of the geometry boundary method. In the context of the material approach, a finite element mesh is fixed in the design domain and the topology optimization is applied to achieve a black (material) and white (void) material configuration pattern in the design space. But it is well known that the optimization problem established in this manner is usually ill-posed and may not converge under a sequence of refining meshes. In this sense, the original problem needs to be relaxed by allowing intermediate density materials. To guarantee a well-posed optimization, a suitable penalty [11] is applied to recover the original binary-like material distribution and an additional numerical scheme such as the filtering method [52,53] should be included to smear out the numerical instabilities [51]. For the geometry-based boundary methods, they can be further classified into two different types, namely the explicit method and the implicit method. The former is usually referred to the classic shape optimization while the latter is mentioned as the level set method. In the classic shape optimization [54], the boundary is usually discretized into a set of parameters which are applied to explicitly control the interface by moving the exterior and interior boundaries. A remeshing procedure is often used to reconstruct the geometrical model periodically when the design boundary crossing elements. The explicit representation is only physically meaningful when the connectivity of the boundary keeps unchanged during the optimization process. To make the topological change possible, the bubble approach [21] or the topological derivative method [55] is usually used for adding new holes inside the structure and then a new shape optimization is possible with a variable topology. The ESO method [70] is also a popularly studied method for structural shape and topology optimization, which is based on an ad hoc criterion to assess each element to the specified objective and subsequently remove those unnecessary elements with the least contributions. In addition, the genetic algorithm (GA) is a widely applied structural optimization method [59]. It is a stochastic search scheme based on the mechanisms of the natural selection and genetics, which codes design variables by mimicking chromosome in biological nature. Perhaps, the ESO and GA methods are more suitable for smaller-scale combined optimization problems with discrete or continuous variables.

The level set method was originally introduced for tracking the evolution process of dynamic interfaces with significantly topological changes in many areas [40,48,41]. It has experienced considerable development with a wide range of applications including fluid mechanics, combustion, computer vision, image processing, material science, and so on [44,58,14]. The success of the level set method can be attributed to the role of curvature in numerical regulation so as to achieve a meaningful vanishing viscosity solution [43]. Recently, the standard level set method has been successfully applied to structural shape and topology optimization problems [49,42,60,2]. Compared to the classic shape optimization, the level set-based optimization is really a family of implicit shape optimization but it is capable of simultaneously implementing topological changes while retaining a smooth boundary. Hence, the level set method is a numerical process of dynamic implicit interfaces that combines the advantages of both the explicit boundary-based method and the material distribution-based method. Sethian and Wiegmann [49] are among the first few researchers who introduced the level set method [40,48] into structural optimization area, in which shape fidelity and topology changes are achieved in accordance with the equivalent stresses along the boundary. Osher and Santosa [42] presented a level set method for topological shape design of an inhomogeneous drum membrane, where the resonant frequency was optimized as the objective function and a project gradient method was utilized to handle the constraint. Wang et al. [60] established the speed vector in terms of the boundary shape and the variation sensitivity as a physically meaningful link between the shape derivative [54] and the powerful level set method [48]. This method was further developed as a “color” level set method to address shape and topology optimization in a multi-material design domain [61]. Allaire et al. [2] independently proposed a similar level set method for structural shape and topology optimization, where the front velocity was derived from a strict shape sensitivity analysis and the front propagation was advanced via the Hamilton–Jacobi PDE, and followed by extended applications [3].

The standard level set method [60,2] shows the potential in implementing many different types of structural shape optimization problems with drastic topological changes. However, there still remain some drawbacks: (1) its final design highly depend on the initial guess as no mechanisms have been included to generate new holes inside the design domain and (2) the time step must be small enough to satisfy the CFL condition, leading to a time-consuming optimization process with hundreds of iterations. To enable the introduction of new holes, the topological derivative method [13,28] has been incorporated into the level set method for the sake of generating new holes. The notion of topological derivative may be initially introduced by [55] to measure the influence of the “nucleation” of small holes inside the design domain. Novotny et al. [39] proposed an alternative definition for the topological derivative and introduced a shape sensitivity analysis method based on the concept of shape derivative [29,54]. Although the level set methods with the topological derivative can produce new holes during optimization process, but it is difficult to switch meaningfully between the topological and the shape derivatives [62,4]. To cut the computational cost relevant to the CFL condition, several alternative level set methods have been developed without directly solving the Hamilton–Jacobi PDE. Such as, Belytschko et al. [8] proposed a level set method for topology optimization with implicit function and regularization, where the node values of the level set function are directly updated with an ad hoc scheme within a narrow band of the zero level set. Haber [24] employed a variant level set method for structural eigenvalue shape optimization combining the sequential quadratic programming method with a multilevel grid refinement method [6] to advance the implicit shape boundaries. Amstutz and Andra [5] proposed a level set-based topology optimization method with the concept of topological gradient. Chen et al. [16] combined R-functions with B-spline functions to present an implicit shape optimization method with parametric control and topological changes. Wang et al. [64,65] proposed an implicit free boundary parameterization method for shape and topology optimization. Wei and Wang [66] presented an alternative scheme for structural shape and topology optimization with the piecewise constant level set method [57,30], which is perhaps more promising in multi-phases topology optimization problems. Based on the contributions of [38,63], Luo et al. [33] presented a new level set method for compliant mechanism designs using the compactly supported radial basis function. In doing so, the original more difficult shape and topology optimization problem driven by the Hamilton–Jacobi PDE is fully parameterized into an easier size optimization of the expansion coefficients, to which many well-founded gradient-based mathematical programming methods such as [56] and optimality criterion based algorithms such as [45,71] can be applied.

The aim of this study is to introduce an alternative level set method for the level set equations with the additive operator splitting (AOS) scheme instead of the explicit schemes. The concept of the semi-implicit AOS algorithm originally rooted from the splitting up method [31] and nonlinear diffusion filtering problems in image analysis [67]. It can be found that many approaches for nonlinear diffusion filtering are based on the finite difference discretization by means of explicit schemes [68]. Compared to the time steps of explicit schemes limited by a restrictive CFL condition (more rigorous for the higher-dimensional cases) [26], the semi-implicit discretization to be presented satisfies all discrete scale-space criteria for all time steps. It can be implemented easily in arbitrary dimensions and reveal a computational complexity and memory requirement being linear in the number of grid points [68]. We are trying to combine the semi-implicit AOS scheme [31,67] with the standard level set method [48,41] to develop a new level set method for structural shape and topology optimization. In doing so, some unfavorable numerical features in the conventional level set method [32,33], such as the CFL condition, the reinitialization procedure and the velocity extension algorithm are expected to be reasonably avoided. In particular, new holes can be created freely inside the material domain which helps the final design get rid of trapped local optimums. In addition, the suggested method is mathematically well-established and can be easily extended to more complicated engineering applications as a general optimization scheme. The recent developments in level set methods [6,24,14,18,25] show that the implicit (or equivalent) schemes are faster than explicit time-marching schemes applied in standard level set methods. It is interesting to test all the different schemes to find the best efficient level set method. However, it is difficult for us to numerically implement and compare all the different schemes with the present semi-implicit level set method. Hence, this work only focus on the comparison with the popularly studied standard level set method [48,42,43,60,2]. Further study will be conducted to compare the present semi-implicit level set method with other level set methods (e.g. [6,24]).

**2. Implicit level set representation**

The basic idea behind the level set representation is expressing a curve or surface as the zero level set or isophote of a high-dimensional function in an implicit manner, and then traces the deformation of the curve or surface via the evolvement of the higher-dimensional level set function [48]. As shown in Fig. 1a, where  $D$  is a fixed working domain which includes all admissible shapes  $\Omega$  (a smooth bounded open set). Fig. 1b is the level set model showing that a 2D interface can be represented with a 3D scalar level set function, which is a signed distance function being Lipschitz continuous. Supposing the level set function  $\Phi(x)$  is defined as

$$\begin{cases} \Phi(x) > 0 \iff \forall x \in \Omega/\partial\Omega & \text{(inside the domain)} \\ \Phi(x) = 0 \iff \forall x \in \partial\Omega & \text{(on the boundary)} \\ \Phi(x) < 0 \iff \forall x \in D/\Omega & \text{(outside the domain)} \end{cases} \quad (1)$$

where  $\Phi(x) > 0$ ,  $\Phi(x) < 0$  and  $\Phi(x) = 0$  denotes the solid, void and boundary, respectively.

In structural optimization, the boundary  $\partial\Omega(x)$  of  $\Omega(x)$  is represented as the zero level set

$$\partial\Omega(x) = \{x \in \mathbb{R}^d | \phi(x) = 0\} \quad (d = 2 \text{ or } 3) \quad (2)$$

Letting the level set function evolve dynamically in time  $t$  with a normal velocity, then the motion of the structural boundary can be expressed as follows:

$$\partial\Omega(t) = \{\Phi(x(t), t) = 0\} \quad \forall x(t) \in \partial\Omega(t) \quad (3)$$

Differentiating Eq. (3) with respect to  $t$  on both sides yields

$$\frac{\partial\Phi}{\partial t} + \frac{dx}{dt} \cdot \nabla\Phi = \frac{\partial\Phi}{\partial t} + v \cdot \nabla\Phi = 0 \quad (4)$$

Consider a normal velocity  $v_n = v \cdot n$  with an outward defined direction  $n = \nabla\Phi/|\nabla\Phi|$ , then the Hamilton–Jacobi PDE can be defined as [48,43]

$$\frac{\partial\Phi(x, t)}{\partial t} + v_n |\nabla\Phi| = 0, \quad \Phi(x, 0) = \Phi_0(x) \quad (5)$$

As a result, the evaluation of the dynamic boundary can be implemented via the level set equation given in (5). It is noted that both the variations of the reference domain  $D$  and the shape boundary  $\partial\Omega$  have been involved. If the velocity  $v_n$  on the boundary is known, transporting  $\Phi$  by the level set model is equivalent to moving the boundary  $\partial\Omega$  along the normal direction.

In general, an analytical function for the scalar level set function is unknown. Hence, a numerical procedure is often indispensable to enable the discrete level set processing, such as an explicit finite difference scheme with a capturing Eulerian approach [43]. However, as noted in [35], the Hamilton–Jacobi type PDE is rarely easy to implement. Several numerical considerations should be handled carefully during the numerical implementation [33], such as the upwind schemes, the reinitialization procedures and the velocity extension algorithms [48].

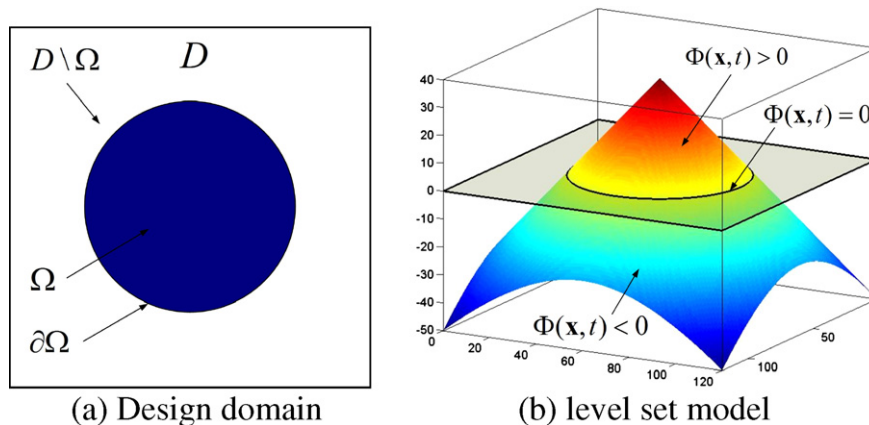


Fig. 1. Level set description of a two-dimensional design.

For the explicit time-marching schemes, the time-step size must be sufficiently small to satisfy the CFL condition and guarantee the convergence of the numerical process [48]. With a fixed Eulerian grid, the CFL condition requires the boundary to move no more than one grid size each time. In applying polynomial interpolation in high dimensions, the mesh grid is required to be sufficiently fine to accurately capture the spatial partial derivative so as to avoid numerical artifacts contaminating the solution [7,15], because only the continuity of the implicit scalar function rather than its partial derivative can be guaranteed crossing the meshing grids. The numerical truncation errors related to the polynomial snaking phenomena may lead to a singular problem as a result of the poor derivative estimation. However, a fine mesh will denote an expensive computational cost with a large amount of iterations if an explicit scheme is adopted, and too much iteration will in turn degenerate the numerical stability due to the accumulation of truncation errors. Thus, the CFL condition should be relaxed as much as possible. Furthermore, the Hamilton–Jacobi PDE is prone to losing its shape in under-resolved regions [20] or unwanted dissipation of the front [50], leading to a too flat or steep level set surface. Hence, some numerical schemes are generally required to be included to retain the regularity of the level set function [18,19,47,58]. A reinitialization procedure is usually included to retain a signed distance level set function to appropriately capture the geometric shape [43]. It was noted that the global reinitialization procedure is usually computational expensive and also prohibit the “nucleation” of new holes inside the material domain [13,2]. The final design will become strongly dependent on the initial guess and the optimization may easily run into local minimums [60,24]. Hence, the global reinitializations should be avoided to save computational cost and also to enable the probability of creating new hole. In addition, the original velocity field in the Hamilton–Jacobi PDE is evaluated only on the boundary via the shape sensitivity analysis methods [54,17]. However, to enable the dynamic level set process in a fixed Eulerian grid, the velocity field is often required to be extended to a narrow band of the boundary or to the entire design domain [2,23,43,48]. Hence, the numerical considerations of the discrete computation limit the application of the level set method to structural shape and topology optimization.

In this study, the structural boundary is still described as the level set equation by fully taking advantage of the implicit free boundary representation [32,60,61]. In doing so, we present an alternative level set method for shape and topology optimization based on a semi-implicit scheme rather than the explicit difference scheme.

### 3. Shape and topological optimization

In the conventional shape and topology optimization, the problem of structural stiffness design has been widely studied. With the level set method, the standard notion of the structural design problem of minimum compliance [12] can be specified as

$$\begin{cases} \text{Minimize :} & J_\Phi(\Omega) = \frac{1}{2} \int_D [D_{ijkl} \varepsilon_{ij}(u) \varepsilon_{kl}(u)] H(\Phi) d\Omega \\ \text{Subject to :} & a_\Phi(u, v) = l_\Phi(v), \forall v \in \mathbf{U}, u|_{\partial\Omega} = u_0 \\ & V(\Omega) = \int_D H(\Phi) d\Omega - V_{\max} \leq 0 \end{cases} \quad (6)$$

where  $J_\Phi$  is the objective functional and  $V$  is the inequality constraint to limit the maximal material usage  $V_{\max}$ . Here, the solid domain  $\Omega$  included in the reference domain  $D$ .  $H(x)$  is Heaviside function and its derivative is defined as Dirac function  $\delta(x)$  [48,43].

$$H(x) = \begin{cases} 1 & \text{if } x \geq 0 \\ 0 & \text{if } x < 0 \end{cases}, \quad \delta(x) = \frac{dH}{dx} \quad (7)$$

The energy bilinear and the load linear forms  $a_\Phi(u, v)$  and  $l_\Phi(v)$  are, respectively, given by

$$a_\Phi(u, v) = \int_D D_{ijkl} \varepsilon_{ij}(u) \varepsilon_{kl}(v) H(\Phi) d\Omega \quad (8)$$

$$l_\Phi(v, \Omega) = \int_D f v H(\Phi) d\Omega + \int_D p v \delta(\Phi) |\nabla \Phi| d\Omega \quad (9)$$

where the elastic equilibrium equation is written in its weak variation form.  $u$  denotes the displacement field and  $v$  is virtual displacement field in the space  $\mathbf{U}$  spanned by kinematically admissible displacement fields,  $D_{ijkl}$

is the elasticity tensor,  $\varepsilon$  represents the strain tensor,  $p$  denotes the body force,  $f$  is the boundary tractions applied on the part  $\partial\Omega_t$  of the boundary  $\partial\Omega$ , and  $u_0$  is the prescribed displacement on the part  $\partial\Omega_u$  of the  $\partial\Omega$ . The aim of the structural optimization is to find the optimal boundary  $\partial\Omega$  of  $\Omega$ , so that the objective function  $J_\phi(u)$  can be minimized for a specific physical or geometric type described by  $\Phi$  [60].

In solving the optimization problem (6), the inequality volume constraint is usually difficult to be exactly satisfied during the level set processing. In the literature, a fixed Lagrange multiplier was appointed to satisfy the volume constraint [2] despite the fact that the constraint is difficult to be satisfied because the multiplier is fixed during the entire optimization process. Another approach was under the assumption that the volume constraint is conservative during the interface propagation [60], but actually the volume cannot be kept conservative as the level set surface is prone to leading to the drift of the volume during the optimization process [20,18]. Therefore, in numerical implementation, it is necessary to accurately calculate the Lagrange multiplier  $\lambda$  (in Eq. (25)) so that the design is always in the feasible domain by pushing the volume violation back. In this study, the augmented Lagrange multiplier method [37] is used to calculate the Lagrange multiplier  $\lambda$ , which is a mathematically well-founded method being widely used in design optimization community. It has been proved to be effective in retaining the volume conservative [66].

#### 4. Shape sensitivity analysis

In this section, the concept of the shape derivative [17,29,54] is viewed as a gradient-based method to guarantee minimization of optimization problem (6). In the framework of Murat and Simon [36], we employ the shape derivative to measure the sensitivity of boundary perturbations with respect to pseudo-time by following a similar way of Wang et al. [60] and Allaire et al. [2]. First, supposing  $\Omega$  is a smooth open set, we consider the following type of domain

$$\Omega_\vartheta = (Id + \vartheta)(\Omega) \tag{10}$$

where  $Id$  is the identity map and  $\vartheta:R^d \rightarrow R^d$  is a small regular mapping operation. Then, if  $\vartheta$  is sufficient small, the existence of  $G(\vartheta):\Gamma \rightarrow \Gamma$  and  $\Phi(\vartheta):\Gamma \rightarrow R$  can be ensured. Hence

$$(I + \vartheta) \circ G(\vartheta) = I + \Phi(\vartheta)n, \text{ on } \Gamma \tag{11}$$

where  $n:\Gamma \rightarrow S^{d-1}$  denotes the unit outward normal on  $\Gamma$ . The objective  $J(\Omega(t))$  is given as

$$J(\Omega(t)) = J(\Omega) + J'(\Omega)\vartheta \cdot n + o(\vartheta) \tag{12}$$

where  $J'(\Omega)$  is the partial derivative with respect to pseudo-time  $t$ , namely, the shape derivative or the shape gradient that is a continuous linear function belonging to  $W^{1,\infty}(\mathbb{R}^d, \mathbb{R}^d)$ . Considering the integral on the volume of  $\Omega$  or along the boundary of  $\Omega$ , we can obtain the following expressions according to [54,17].

If  $f(x) = W^{1,1}(\mathbb{R}^N)$  and  $\Theta(\Omega) = \int_\Omega f(x)dx$ , then the shape derivative of  $\Theta(\Omega)$  is defined as

$$\frac{\partial\Theta(\Omega)}{\partial t} = \int_\Omega \nabla \cdot (\vartheta(x)f(x))dx = \int_{\partial\Omega} \vartheta(x) \cdot n(x)f(x)ds \tag{13}$$

If  $f(x) = W^{2,1}(\mathbb{R}^N)$  and  $\Theta(\Omega) = \int_{\partial\Omega} f(x)dx$ , then the shape derivative of  $\Theta(\Omega)$  is defined as

$$\frac{\partial\Theta(\Omega)}{\partial t} = \int_{\partial\Omega} \vartheta(x) \cdot n(x) \left( \frac{\partial f(x)}{\partial n} + \kappa f(x) \right) ds \tag{14}$$

In terms of the aforementioned definitions, the shape derivatives of  $J_\phi(\Omega(t))$ ,  $a_\phi(u, v, \Omega(t))$  and  $l_\phi(v, \Omega(t))$  with the level set representation can be, respectively, expressed as

$$\frac{\partial J_\phi(\Omega(t))}{\partial t} = \int_D D_{ijkl}\varepsilon_{ij}(\dot{u})\varepsilon_{kl}(u)H(\Phi)d\Omega + \frac{1}{2} \int_D D_{ijkl}\varepsilon_{ij}(u)\varepsilon_{kl}(u)\delta(\Phi) \frac{\partial\Phi}{\partial t} d\Omega \tag{15}$$

$$\frac{\partial a_\phi(\Omega(t))}{\partial t} = \int_D D_{ijkl}\varepsilon_{ij}(\dot{u})\varepsilon_{kl}(v)H(\Phi)d\Omega + \int_D D_{ijkl}\varepsilon_{ij}(u)\varepsilon_{kl}(\dot{v})H(\Phi)d\Omega + \int_D D_{ijkl}\varepsilon_{ij}(u)\varepsilon_{kl}(v)\delta(\Phi) \frac{\partial\Phi}{\partial t} d\Omega \tag{16}$$

$$\frac{\partial l_\phi(\Omega(t))}{\partial t} = \int_D [f\dot{v} + \text{div}(p\dot{v}n)]H(\Phi)d\Omega + [fv + \text{div}(pvn)]\delta(\Phi) \frac{\partial\Phi}{\partial t} d\Omega \tag{17}$$

In addition, the conjugate equation is defined as follows:

$$\int_D D_{ijkl} \varepsilon_{ij}(u) \varepsilon_{kl}(\dot{v}) H(\Phi) = \int_D [f\dot{v} + \text{div}(p\dot{v}n)] H(\Phi) d\Omega \tag{18}$$

Differentiating  $a_\phi(u, v, \Omega) = l_\phi(v, \Omega)$  on both sides with respect to  $t$ , namely

$$\frac{\partial a_\phi(u, v, \Omega(t))}{\partial t} = \frac{\partial l_\phi(v, \Omega(t))}{\partial t} \tag{19}$$

In terms of  $\partial\Phi/\partial t = \delta(\Phi)|\nabla\Phi|v \cdot n$ , substituting Eqs. (16)–(18) into (19) yields

$$\int_D D_{ijkl} \varepsilon_{ij}(\dot{u}) \varepsilon_{kl}(v) H(\phi) d\Omega = \int_D [fv + \text{div}(pvn) - D_{ijkl} \varepsilon_{ij}(u) \varepsilon_{kl}(v)] \delta(\Phi) |\nabla\Phi| v \cdot n d\Omega \tag{20}$$

The problem of structural mean compliance is being widely accepted as the self-adjoint problem [60,2], which indicates

$$\int_D D_{ijkl} \varepsilon_{ij}(\dot{u}) \varepsilon_{kl}(u) H(\Phi) d\Omega = \int_D [fu + \text{div}(pun) - D_{ijkl} \varepsilon_{ij}(u) \varepsilon_{kl}(u)] \delta(\Phi) |\nabla\Phi| v \cdot n d\Omega \tag{21}$$

By substituting Eq. (21) into (15), the shape derivative of  $J_\phi(\Omega(t))$  is then given as

$$\frac{\partial J_\phi(\Omega(t))}{\partial t} = \int_D \left[ fu + \text{div}(pun) - \frac{1}{2} D_{ijkl} \varepsilon_{ij}(u) \varepsilon_{kl}(u) \right] \delta(\Phi) |\nabla\Phi| v \cdot n d\Omega \tag{22}$$

Similarly, the shape derivative of the volume constraint can be expressed by

$$\frac{\partial}{\partial t} V_\phi(\Omega(t)) = \int_D \delta(\Phi(x)) |\nabla\Phi| v \cdot n d\Omega \tag{23}$$

In this study, the augmented Lagrangian method is applied to convert the original constrained optimization problem into an unconstrained problem as follows:

$$\bar{J}_\phi(\Omega) = J_\phi(\Omega) + \lambda \left[ \int_D H(\Phi) d\Omega - V_{\max} \right] + \frac{1}{2A} \left[ \int_D H(\Phi) - V_{\max} \right]^2 \tag{24}$$

With the augmented Lagrangian multiplier method [8,37], the updating scheme for the Lagrangian multiplier  $\lambda$  relevant to the volume constraint can be obtained as

$$\lambda^{k+1} = \lambda^k + \frac{1}{A^k} \left[ \int_D H(\Phi) - V_{\max} \right], \quad A^{k+1} \in (0, A^k) \tag{25}$$

where  $A$  is the penalization parameter. In numerical implementation,  $A$  is set to a small positive parameter which is decided as  $A^{k+1} = \alpha^* A^k$  with  $\alpha < 1$ . Our numerical tests show that the penalization parameter is stable for structural topology optimization problems if  $\alpha$  can be selected between  $\alpha = 0.1$ – $0.5$ . At least, it performs well for structural stiffness designs. For detailed overview of calculating the Lagrange multiplier, the readers are referred to the related references (e.g. [9,37]).

Thus, the shape derivative of the augmented objective function  $\bar{J}$  can be worked out as

$$\begin{aligned} \frac{\partial \bar{J}_\phi(\Omega(t))}{\partial t} &= \frac{\partial}{\partial t} J_\phi(\Omega(t)) + \frac{\partial}{\partial t} \left\{ \lambda \left[ \int_D H(\Phi) d\Omega - V_{\max} \right] + \frac{1}{2A} \left[ \int_D H(\Phi) - V_{\max} \right]^2 \right\} \\ &= \int_D G(\Phi) \delta(\Phi) |\nabla\Phi| v \cdot n d\Omega \end{aligned} \tag{26}$$

$$G(\Phi) = \left[ fu + \text{div}(pun) - \frac{1}{2} D_{ijkl} \varepsilon_{ij}(u) \varepsilon_{kl}(u) + \lambda + \frac{1}{A} \left( \int_D H(\Phi) - V_{\max} \right) \right] \tag{27}$$

In terms of  $v_n = v \cdot n$ , Eq. (26) can be further written as

$$\frac{\partial \bar{J}_\phi(\Omega(t))}{\partial t} = \int_D G(\Phi) \delta(\Phi) |\nabla\Phi| v_n d\Omega \tag{28}$$

It is noted that the derivative of the augmented objective form will agree with the derivative of the objective functional if all the constraints are satisfied. To ensure the decrease of the objective function, a proper velocity field  $v_n$  should be selected for the level set function. As indicated in the literature [60,2], the simplest way is to directly choose a steepest descent direction by letting

$$v_n = -G(\Phi) \tag{29}$$

Thus, the shape derivative can guarantee a descent direction of the objective function

$$\frac{\partial J_\phi(\Omega(t))}{\partial t} = - \int_D G^2(\Phi) \delta(\Phi) |\nabla \Phi| d\Omega \leq 0 \tag{30}$$

In addition, to ensure a smooth design boundary, the normal velocity field can be modified by adding an artificial regularization term for smoothing purpose [60], namely the velocity field is rewritten as

$$v_N = v_n + \beta \kappa \tag{31}$$

where  $\beta$  is a small positive parameter and  $\kappa = \text{div}(\nabla \Phi / |\nabla \Phi|)$  represents the mean curvature in 2D structures [61].

### 5. A semi-implicit scheme with AOS algorithm

In this study, we use a semi-implicit AOS method rather than explicit schemes to implement the discrete level set processing. It was noted that the conventional semi-implicit schemes can satisfy all discrete scale-space criteria for any time step [26]. But it should be addressed that the numerical procedure for solving higher dimensions linear system will be significantly less efficient. To overcome this shortcoming, the semi-implicit AOS scheme is presented in this study as an alternation. The concept of semi-implicit scheme might be firstly mentioned by [31] and later developed by [67]. The original application of the AOS scheme is to solve nonlinear diffusion equations in image processing and computer vision [67–69]. The basic idea behind the AOS scheme is to split the  $m$ -dimensional spatial operator into a set of one-dimensional space discretizations that can be efficiently solved with a mathematically well-founded Gaussian elimination algorithm named *Thomas Algorithm* [67]. As a result, the final multi-dimensional solution can be approximated via averaging the 1-D solutions. The semi-implicit AOS scheme inherits several favorable features from their original continuous diffusion process. It treats all coordinate axes equally and can be easily implemented in arbitrary dimensions. In addition, this scheme is expected to be fast as due to no time step limitation related to the CFL condition. The computational complexity and memory requirement is linear in the number of pixels.

In the conventional Eulerian method, the nonlinear diffusion filtering problems are usually defined with the following explicit scheme [67]

$$\frac{u_i^{k+1} - u_i^k}{\tau} = \sum_{l=1}^m \sum_{j \in N_l(i)} \frac{g_j^k + g_i^k}{2h_l^2} (u_j^k - u_i^k) \tag{32}$$

where the boundary condition is  $u(x, 0) = u(x)$ ,  $u_i^k$  and  $g_i^k$  are used to approximate  $u(x_i, t_k)$  and  $g(\nabla u_\epsilon(x_i, t_k))$ , respectively,  $N_l(i)$  is the set of the two neighbors of grid points  $i$  along the  $l$  directions and  $m$  denotes the dimension of the problems (2 or 3). Thus, in 2D problems,  $l$  represents  $x$  and  $y$  direction, while in 3D cases it denotes  $x$ ,  $y$  and  $z$  direction, respectively.  $h_l$  is the minimal grid dimension in  $l$  direction, and  $\tau$  is the time step. In matrix–vector notation, the explicit scheme is rewritten compactly as

$$\frac{u_i^{k+1} - u_i^k}{\tau} = \sum_{l=1}^m A_l(u^k) u^k \tag{33}$$

where  $A_l$  is the diffusive interaction in  $l$  direction, which can be defined as follows:

$$A(u^k) = a_{ij}(u^k) = \begin{cases} \frac{1}{2h_l^2} (g_j^k + g_i^k), & j \in N_l(i) \\ 0, & \text{else} \\ - \sum_{n \in N_l(i)} \frac{1}{2h_l^2} (g_j^k + g_n^k), & i = j \end{cases} \tag{34}$$



In general, the above equation is the so-called explicit scheme because the solution can be directly calculated without solving a system of equations, but it is well known that the explicit scheme has a strict limitation on time-marching step size and it is only numerically stable for very small time steps [26,31], which leads to poor computational efficiency and limits its practical applications.

Keeping this in mind, a semi-implicit scheme originally for nonlinear diffusion equations in image processing and computer version was then presented as an alternation [67–69]. We suppose that a filtered image  $u(x, t)$  for an image  $u(x)$  is defined as the solution of the following problem by involving suitable initial state and boundary conditions

$$u(x, t) = a(x)\nabla \cdot \left( \frac{b(x)}{|\nabla u|} \nabla u \right) + \lambda\varphi(x), \quad u(x, 0) = u(x) \tag{35}$$

In the above equation,  $u(x, t)$  represents the filtered scalar image with Gaussian-smoothness, which can be calculated by solving a nonlinear diffusion equation with the original image  $u(x)$  as its initial state [68]. Recalling the definition of the level set function  $\Phi(x, t)$  [48,43], and taking  $a(x) = \beta$ ,  $b(x) = 1$  and  $\lambda\varphi(x) = B(x)$ , then we have the following formulation:

$$\Phi_t = \beta\nabla \cdot \left( \frac{\nabla\phi}{|\nabla\phi|} \right) + B(x), \quad \Phi(x, 0) = \Phi(x) \tag{36}$$

where  $\beta$  is the weighting factor for the diffusion term and  $B(x)$  is decided by different problems.

Discretizing the system with reflecting boundary conditions, the semi-implicit scheme for the level set function is initially expressed in matrix–vector notation form as

$$\frac{\Phi_i^{k+1} - \Phi_i^k}{\tau} = \sum_{l=1}^m \beta A_l(\Phi^k) \Phi^{k+1} + B(x), \quad \Phi^0 = \Phi(x, 0) \tag{37}$$

Here, the “semi-implicit” implies that the level set function  $\Phi^{k+1}$  can not be directly obtained, and we have to solve a linear system first, which leads to the following expression:

$$\Phi^{k+1} = \left[ I - \tau\beta \sum_{l=1}^m A_l(\Phi^k) \right]^{-1} \Phi^k + \tau B(x), \quad \Phi^0 = \Phi(x, 0) \tag{38}$$

It was noted that this scheme theoretically guarantees the stability by satisfying all the discrete scale-space for arbitrary time step sizes  $\tau > 0$  [67].

To solve the aforementioned problem efficiently, let us consider a modification of the semi-implicit scheme, namely the additive operator splitting (AOS) scheme [68]

$$\Phi^{k+1} = \frac{1}{m} \sum_{l=1}^m [I - m\tau\beta A_l(\Phi^k)]^{-1} (\Phi^k + \tau B(\Phi)) \tag{39}$$

where the operators  $B_l(\Phi^k) = [I - m\tau\beta A_l(\Phi^k)]$  indicate one-dimensional diffusion processes along the  $x_l$  axes. Under the condition of a conservative pixel numbering in the  $l$  direction, all these operators are composed of a strictly diagonally dominant tridiagonal linear system. It is noted that the AOS scheme has the same first-order Taylor expansion in  $\tau$  as the semi-implicit scheme.

Substituting the velocity  $v_N$  in Eq. (31) into the level set model in Eq. (5) leads to

$$\Phi_t = \beta|\nabla\Phi|\text{div}\left(\frac{\nabla\Phi}{|\nabla\Phi|}\right) + |\nabla\Phi|v_N \tag{40}$$

According to Eqs. (36) and (37), the formulation (40) can be re-expressed as

$$\frac{\Phi_i^{k+1} - \Phi_i^k}{\tau} = \beta|\nabla\Phi^k|[A_l(\Phi^k)\Phi^{k+1}] + v_N|\nabla\Phi^k| \tag{41}$$

Then, with the AOS scheme given in Eq. (39), the level set function  $\Phi$  can be updated in terms of the following manner:

$$\Phi^{k+1} = \frac{1}{m} \sum_{l=1}^m [I - m\tau\beta|\nabla\Phi^k|A_l(\Phi^k)]^{-1}[\Phi^k + \tau(v_N(x)|\nabla\Phi^k|)] \quad (42)$$

with the definition of  $A_l(\Phi^k) = a_{ij}(\Phi^k)$ , and  $a_{ij}(\Phi^k)$  can be expressed as

$$a_{ij} = \begin{cases} \frac{1}{h_i^2} \frac{2}{(|\nabla\Phi_i^k| + |\nabla\Phi_j^k|)}, & j \in N_l(i) \\ 0, & \text{else} \\ -\frac{1}{h_i^2} \sum_{n \in N_l(i)} \frac{2}{(|\nabla\Phi_i^k| + |\nabla\Phi_n^k|)}, & i = j \end{cases} \quad (43)$$

The operator  $A$  can be split into two components in  $x$  and  $y$  directions (2D), respectively, as

$$A_1 = \frac{\partial}{\partial x} \left( \frac{1}{|\nabla\Phi^k|} \frac{\partial}{\partial x} \right), \quad A_2 = \frac{\partial}{\partial y} \left( \frac{1}{|\nabla\Phi^k|} \frac{\partial}{\partial y} \right) \quad (44)$$

In numerical implementation, the level set function  $\Phi$  can be updated as

$$\Phi^{k+1} = \frac{1}{2} [(I - 2\tau\beta A_1(\Phi^k))^{-1} + (I - 2\tau\beta A_2(\Phi^k))^{-1}] [\Phi^k + \tau v_N(x)|\nabla\Phi^k|] \quad (45)$$

To simplify the above equation, let

$$\Psi_1(\Phi) = (I - 2\tau\beta A_1(\Phi^k))^{-1} [\Phi^k + \tau v_N(x)|\nabla\Phi^k|] \quad (46)$$

$$\Psi_2(\Phi) = (I - 2\tau\beta A_2(\Phi^k))^{-1} [\Phi^k + \tau v_N(x)|\nabla\Phi^k|] \quad (47)$$

Then,  $\Psi_1(\Phi)$  and  $\Psi_2(\Phi)$  can be easily solved with the following equations using the *Thomas method* as a Gaussian elimination algorithm for tridiagonal systems [67].

$$[I - 2\tau\beta A_1(\Phi^k)]\Psi_1(\Phi) = \Phi^k + \tau v_N(x)|\nabla\Phi^k| \quad (48)$$

$$[I - 2\tau\beta A_2(\Phi^k)]\Psi_2(\Phi) = \Phi^k + \tau v_N(x)|\nabla\Phi^k| \quad (49)$$

With many numerical demonstrations, we can find that the AOS scheme is at least as ten times efficient as the widely used explicit schemes under appropriate requirements. The AOS scheme does not suffer from any practical time step size restriction due to total relaxation of the CFL condition, but it suggested that in practice it is unnecessary to use an impractically large time step, as it will lead to poor rotation invariance in nonlinear diffusion problems [67]. Strictly speaking, the AOS scheme is numerically not unconditionally stable due to the linearization used in the scheme. Hence, selecting the time step needs a practical consideration, this is because a too large time step will influence structural topology complexity and will cause oscillations from the large changes of the structure volume. In any sense, the present scheme can really enable a larger time step and can eliminate the time-consuming reinitialization procedures.

## 6. Numerical implementation

### 6.1. Numerical skills

In level set-based structural topology optimization method, the structural geometric boundary to be optimized is described as the zero level set of  $\Phi(x, t) = 0$ . In its numerical implementation, after obtaining the nodal value of the level set function using the AOS scheme, the level set function  $\Phi$  can be represented in any convenient form as long as it can satisfy the basic requirement [48]. In this work, the finite element method is employed in discrete level set processing with the Heaviside function defined as follows [60]:

$$H(x) = \begin{cases} 0, & x < -\eta \\ \frac{1}{2} \left[ 1 + \frac{x}{\eta} + \frac{1}{\pi} \sin \left( \frac{\pi x}{\eta} \right) \right], & |x| \leq \eta \\ 1, & x > \eta \end{cases} \tag{50}$$

where  $\eta$  is a parameter used to determine the size of the bandwidth for the purpose of numerical smoothness. In our research, it is selected as 0.5 times of the minimum grid width.

To facilitate numerical process using the standard finite element method, the strain field can be calculated without time-consuming remeshing procedure by using the popular and simple “ersatz material” method [2]. In the “ersatz material” scheme, the void holes inside the design domain is filled with a weak material and the element stiffness crossing the boundary is handled under the assumption that it is approximately proportional to the area-fraction of solid materials.

As aforementioned, the AOS method can be regarded as a time stable semi-implicit scheme to solve the level set equation which is mathematically defined as the Hamilton–Jacobi PDE. However, in numerical implementation, a practical max–min constraint should be included in calculating  $|\Delta\Phi|$  so as to guarantee the numerical stability, which can be defined as

$$|\nabla\Phi| = \min(1e4, \max(|\nabla\Phi|, 1e - 4)) \tag{51}$$

In addition, we also need to regularize the velocity field [60] by letting

$$v_N = v_N / \max(|v_N|) \tag{52}$$

### 6.2. Numerical examples

Two widely studied examples in structural topology optimization are used to illustrate the potentials of the present semi-implicit level set method. In all the examples, an artificial material is adopted only for the sake of simplicity [52]. However, it is straightforward to apply the present semi-implicit level set method to structural shape and topology optimization problems including any kinds of engineering materials. The units of all the parameters can be defined flexibly, but they should remain unchanged during all different stages such as formulation modeling, numerical calculation and optimization procedure. In this research, the material properties are defined as: Young’s modulus for solid component is  $E = 1$  and for weak part is  $E = 0.0001$ , and the Poisson ratio for all the materials is  $\nu = 0.3$ . The level set function is initially embedded as a signed distance function, but no reinitializations are required in the rest of iterations. The termination criterion of iteration is the relative difference of the objective function values between two successive iterations is less than 0.0015.

#### 6.2.1. Michell type structure

The well-known Michell type structure with a length and width ratio of 2:1 is used as the first numerical case. The reference domain and the initial design of the structure are shown respectively in Figs. 2 and 3. The structure is loaded with a concentrated vertical force of  $F = 1$  at the centre of the bottom edge, and it

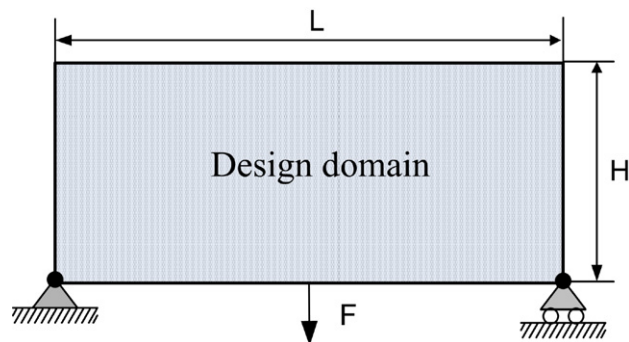


Fig. 2. Design domain with boundary condition.

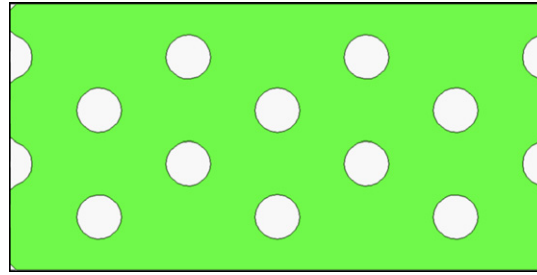


Fig. 3. The initial design of Michell type structure.

is supported on rollers at the bottom-right corner and on fixed supports at the bottom-left corner. The design domain is discretized with  $80 \times 40$  finite elements. The Lagrange multiplier is correspondingly updated together with the level set function, and the positive number is selected as  $\lambda = 0.1$ . For comparison purpose, the initial design displayed in Fig. 3 is optimized by using the proposed semi-implicit AOS scheme and the standard explicit scheme [60], respectively.

Fig. 4 illustrates the designs in different stages of the optimization process using the semi-implicit AOS scheme with a time step  $\Delta\tau = 15$  and a mean curvature coefficient  $\beta = 1e-6$ . The final design shown in Fig. 4f is obtained after 60 iterations. To benchmark the present level set method, we also apply the explicit time-marching (upwind) scheme [34] to solve the same initial design with the same convergent tolerance. From the designs displayed in Fig. 5, one can find that the two different schemes can lead to similar designs. However, to ensure the stability of the explicit scheme, the time step size in upwind method has to be set to 0.5 in the numerical process in order to meet the CFL condition as recommended in the literature [60,2]. Fig. 5f shows the final design obtained after 1162 iterations. The results obtained with the two different difference schemes are listed in Table 1, respectively, where  $N$  is the total number of steps,  $T_s$  denotes the total time of the optimization,  $t_{ls}$  is the average time of one the level set iteration, and  $t_{FEM}$  is the average time of one FEM iteration.

In Table 2, it can be seen that the present algorithm with AOS scheme is more efficient than the conventional or standard level set method with explicit schemes, because the present semi-implicit scheme is mostly time-stable for any time step sizes, thus allowing a bigger time step. In the AOS scheme, the only thing in selecting the time step is a practical consideration, as we addressed previously. A time step which is impractically large will influence the topological complexity of the final design [27]. At the same time, if a too big time step size is applied, our numerical tests show that the objective function and the volume ratio may experience slight oscillation, in particular, near the optimal point. Perhaps, the reason being responsible for this phenom-

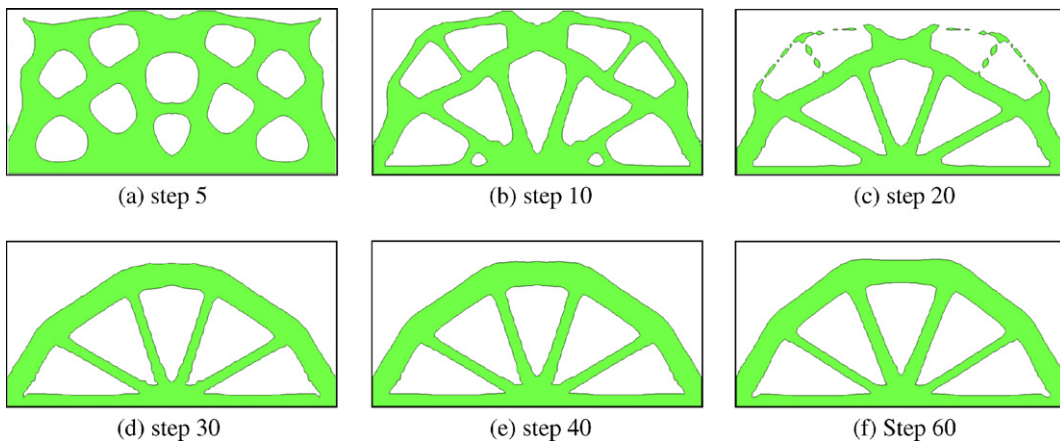


Fig. 4. Designs using the semi-implicit AOS scheme.

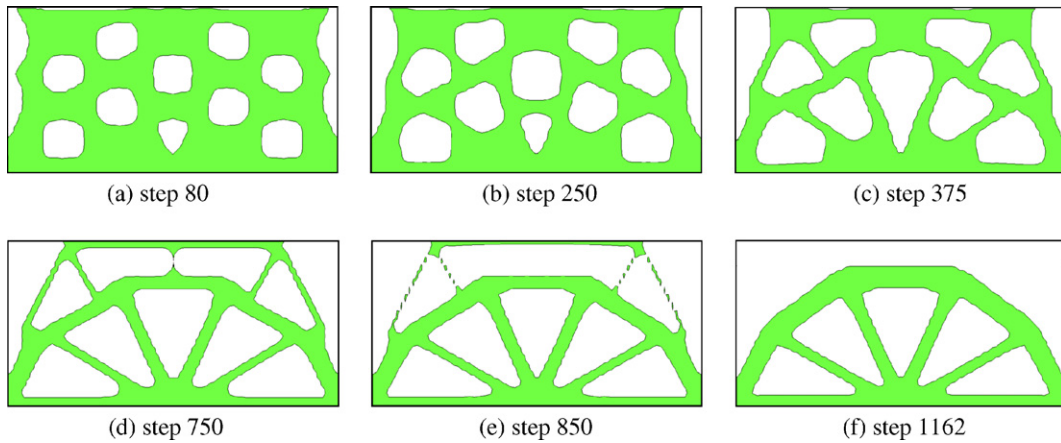


Fig. 5. Designs using the explicit upwind scheme.

Table 1  
Comparison of the explicit upwind and the semi-implicit AOS scheme

Schemes	$J (\Omega)$	$t_{ls}$ (s)	$t_{FEM}$ (s)	$N$	$T_s$ (s)
AOS scheme	18.690	0.01	5.12	60	326.74
Upwind scheme	19.635	0.1	5.09	1162	1256.73

Table 2  
Results of the different designs

Initial design	$J (\Omega)$ (objective)	$T_s$ (s) (total time)	$N$ (iterations)
Fig. 8a with seven holes	75.46	636.64	120
Fig. 9b with three holes	78.54	933.46	183
Fig. 10c without hole	77.87	1297.75	257

enon is that a very large time step will lead to an abrupt change of the structure volume. Hence, the pre-knowledge from a few numerical tests is generally required in order to determine a more suitable time step in advance, if the present level set method is applied.

In the numerical implementation, it was noticed that the computational cost for the FEA analysis is more expensive than the Hamilton–Jacobi PDE [60]. In the conventional level set method, the level set surface (in 2D) is advanced slowly with very small time steps due to the consideration of the CFL condition. Hence, to reduce the FEA cost, only one FEA subroutine is often performed every five level set evolutions [2]. However, in the present semi-implicit AOS scheme, the FEM analysis is performed together with the level set motion every time, because the present scheme enables a quick evolution of the level set surface via a much bigger time step size. However, the total time of the present level set method with the AOS scheme is still much less than the conventional level set method.

Fig. 6a shows that the convergent curves of the objective function and the volume ratio. At first appearance, it seems that the objective function is optimized in opposite direction being inconsistent with what we have expected, but it is truly reflect the changing tendency of the objective function during the entire optimization process. It can be found that the strain energy of the objective function gradually increases from 12.790 to 22.532 in the initial 30 iterations, which is in fact due to the violation of the volume constraint at the initial stage. After that, the objective function smoothly decreases from 22.532 to 18.690 until the design converges to a (local) minimum. The volume constraint of the present method can be exactly satisfied after the 30th iteration, which shows that the augmented Lagrange method can be applied to make the volume conservative. Fig. 6b displays the optimization histories of the objective function and the volume constraint when the

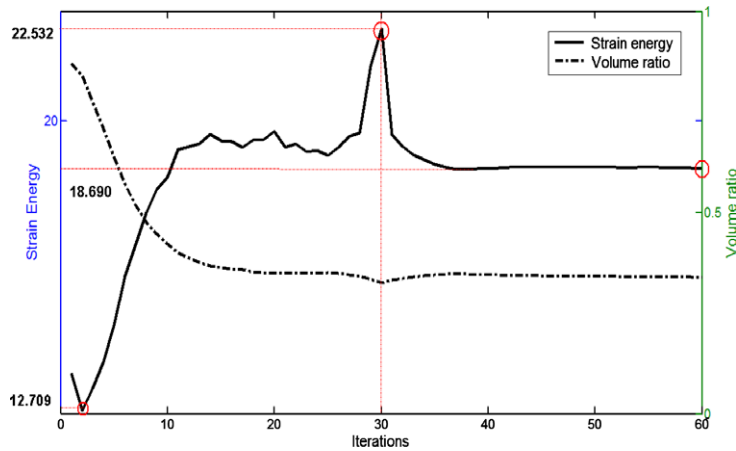


Fig. 6a. The strain energy and the volume ratio with the AOS scheme.

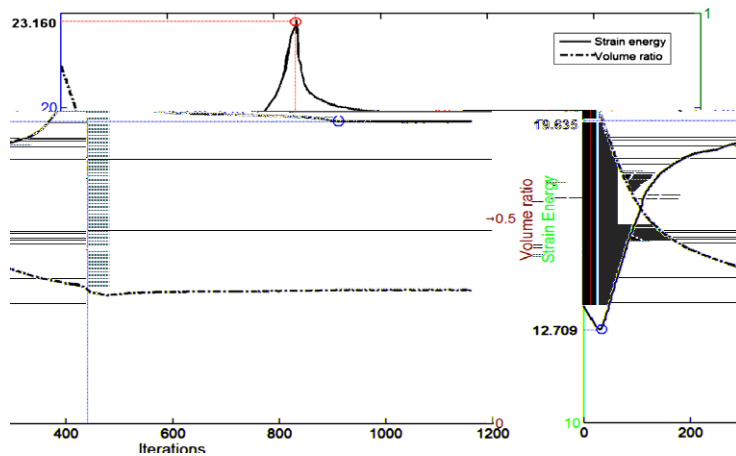


Fig. 6b. The strain energy and the volume ratio with the upwind scheme.

conventional level set method with explicit upwind scheme is employed. In the initial 421 iterations, the strain energy of the objective function increases from 12.709 to 23.160, and then followed with a descent from 23.160 to 19.635.

6.2.2. Cantilever beam

The design domain of a cantilever beam is shown in Fig. 7. The design domain  $D$  is discretized with a rectangle of size  $2 \times 1$  with a fixed boundary on the left side, and a unit vertical load  $F$  is applied at the bottom point of the right side. This example is applied to illustrate some other characters of the semi-implicit AOS scheme in the level set-based structural shape and topology optimization. In all the numerical cases, we use a quadrilateral mesh of  $80 \times 40$  elements, the mean curvature coefficient and the time step size for the AOS scheme will be addressed.

(1) Influence of different initial designs

In the conventional level set method [60,2], in order to obtain a meaningful design, the number of the holes positioned inside the initial design should be topologically sufficient to include all the possible shape configurations. However, in the conventional level set method, no mechanisms have been included to create new holes inside the material domain [4,13,62]. Hence, the final design becomes strongly dependent on

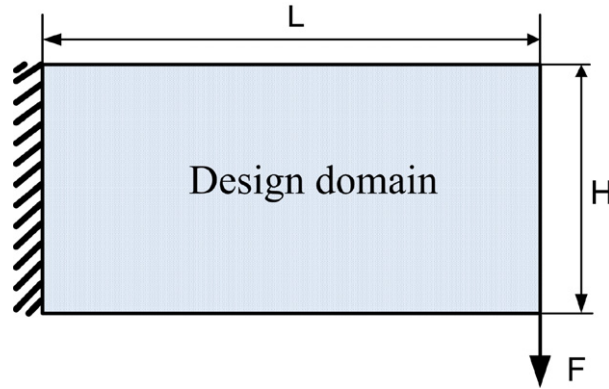


Fig. 7. The cantilever beam boundary condition.

the initial guess, and the design will be easily trapped into local minima. Perhaps, many reasons can be responsible for the prohibition of generating new hole inside the design domain [32]. As far as the level set method with the Hamilton–Jacobi PDE is concerned, a widely recognized reason is that the continuously applied reinitializations for the level set surface (in 2D) has disabled “nucleation” of the new holes [60,2]. To some extent, in the present method, the global reinitializations can be eliminated, and the velocity field is being naturally extended over the entire design domain and the shape gradient is also evaluated on the whole domain.

According to our engineering knowledge, the number of seven holes positioned in the initial design in Fig. 8 should be sufficient to illustrate all the topological configurations. The final design in Fig. 8 is similar to the design obtained using SIMP approach [52] or the conventional level set method [60]. In Fig. 9, the three holes are insufficient topologically to describe a well accepted optimal solution. However, due to the present method being able to create new holes freely, the optimization processing finally leads to a similar design being achieved via adding and deleting holes freely during the optimization. To further demonstrate the capability of the present method, the optimization is performed without putting any hole in the initial design. In Fig. 10, from the optimization procedure, it can be found that the present level set method can freely generate new holes inside the design domain. As a result, a final design in Fig. 9 is achieved with a similar topology as the previous two cases in Figs. 7 and 8. Thus, these three different initial cases can result in similar designs via simultaneous shape fidelity and topological changes. The reason is that the level set method in this paper can create new holes flexibly inside the design domain, which makes the final design highly independent of the initial design. Therefore, the present method with the AOS scheme is

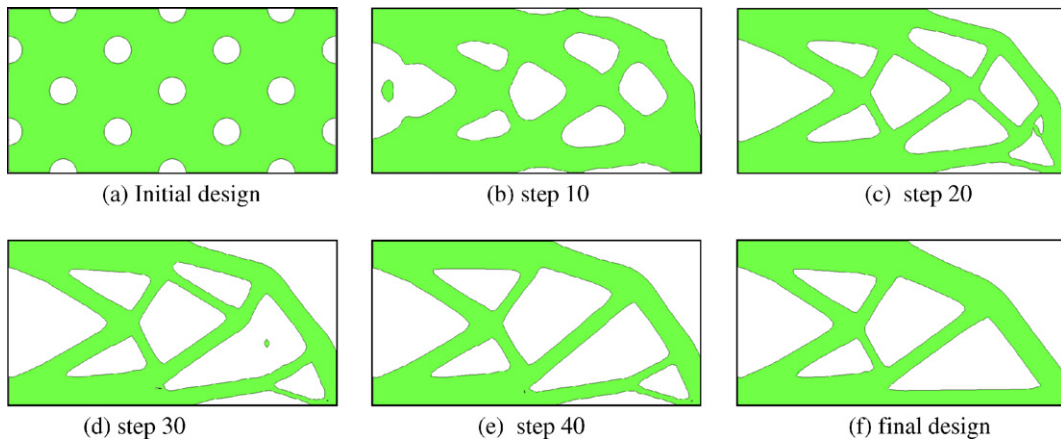


Fig. 8. Design in different stages with seven holes in the design domain.

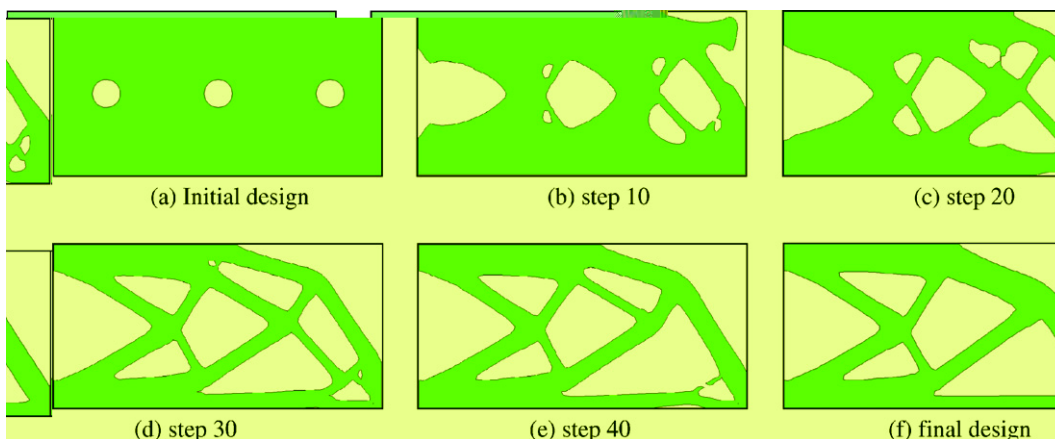


Fig. 9. Design in different stages with three holes in the design domain.

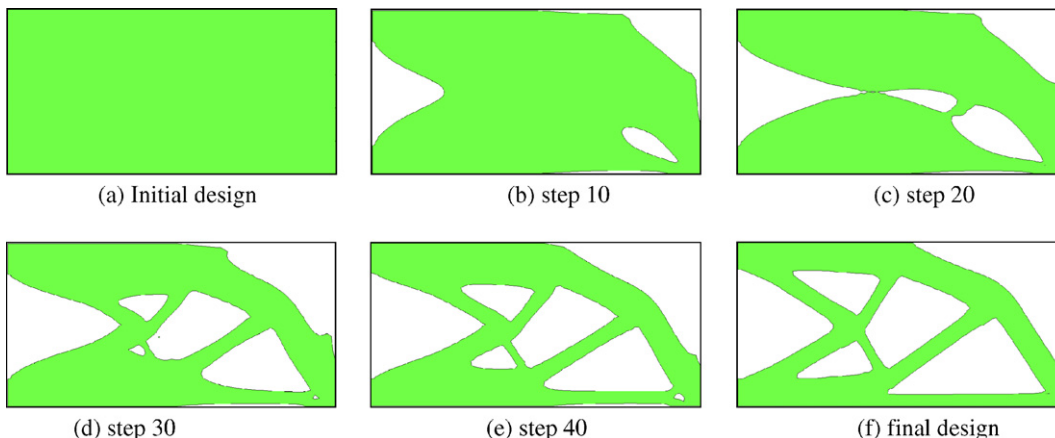


Fig. 10. Design in different stages with three holes in the design domain.

promising for structural shape and topology optimization problems. The results of the different designs are shown in Table 2.

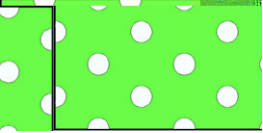
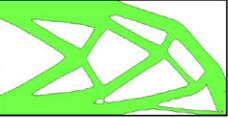

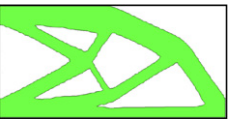
For the conventional level set method using the explicit upwind scheme, it is well known that the initial design has an obvious influence on the final design because the optimization process can not introduce new holes. To overcome the shortcoming, a bubble [21] or topological gradient method [13] is often incorporated into the level set method for the purpose of inserting new holes in the design domain. But it was noted that it would be difficult to switch physically between the topological derivative and the shape derivative in an automatic manner [62,4]. In this sense, the ability of the creation of new holes (at least in 2D) by merging or splitting the boundary can be regarded as a main advantage of the present level set method over the conventional or standard level set method [60,2]. In addition, the present scheme does not need to perform periodical reinitializations to retain the regularization of the level set surface.

#### (2) Influence of the curvature coefficient

In the semi-implicit AOS scheme, the curvature coefficient  $\beta$  is an important parameter. Hence, three numerical cases are used to demonstrate the influence of the curvature coefficient  $\beta$  on final designs. All the optimization results are obtained by using the same initial design with a quadrilateral mesh of  $80 \times 40$  and a step size of 1. The optimal results and relevant topologies are shown in Table 3, where  $\beta$  is the coefficient of the curvature,  $N$  represents the number of total iterations and  $T_s$  denotes the total time.



Table 3  
Results with different curvature coefficient

Initial design	$J(\Omega)$	$\beta$	$T_s$ (s)	$N$	Final design
	74.94	$1e-7$	3875.53	746	
	76.46	$1e-6$	1721.47	352	
	78.64	$1e-5$	527.43	110	

From Table 3, it can be seen that the different curvature coefficients will result in the different final designs. Hence, the curvature coefficient in the semi-implicit AOS scheme has a notable influence on final designs. The numerical results indicates that the larger the coefficient, the simpler the topology of the final design, and the faster the convergence speed. So the curvature coefficient may also be called perimeter constraint similar to that in the reference [61].

6.2.3. Influence of the step size

In solving the Hamilton–Jacobi PDE with the semi-implicit AOS scheme, another important parameter is the time step size  $\Delta\tau$ . We apply three different numerical cases to explore the influence of the time step on final design. The same initial design with a quadrilateral mesh of  $80 \times 40$  and a mean curvature coefficient of  $1e-6$  is adopted. The optimal results are listed in Table 4. It can be seen that the time step size in the AOS scheme has an obvious influence on the final designs. As aforementioned, the semi-implicit AOS scheme is stable with all time steps, and this statement is meaningful only with respect to the time-marching schemes for the Hamilton–Jacobi PDE. Although the present method is free from time step restriction on solving initial value problems, this numerical test displays that the time step really has an impact on the final designs. As a matter of fact, the observation on  $\tau$  is easy to understand because  $\tau$  used in the AOS scheme has a role similar to the

Table 4  
Results with different step size

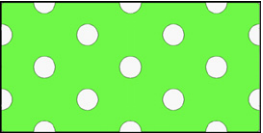
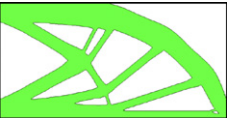

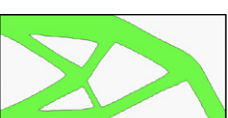
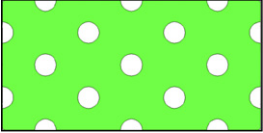

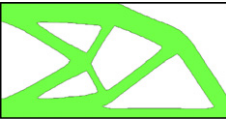
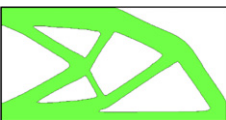
Initial design	$J(\Omega)$	$\tau$	$T_s$ (s)	$N$	Final result
	73.57	0.5	3806.67	750	
	75.47	5	1012.43	193	
	78.32	15	512.52	102	

Table 5  
Results with different step size

Initial design	$J(\Omega)$	mesh	$T_s$ (s)	$N$	Final design
	74.96	$80 \times 40$	616.6	136	
	74.68	$120 \times 60$	10881.5	386	
	74.84	$160 \times 80$	20516.8	637	

moving limit in the SIMP approach [27,52]. In general, a too large step size may weaken the capability of the optimization method in describing topologies of sub-structures in optimization process. In particular, it may remove the basic structure to have included the optimal topology configuration within the initial iterations. In Table 4, it is evident that larger time step size yields a final design of simpler topology. The larger the step size, the larger the change in the nodes' values of the level set function, and then the simpler the final topology.

To demonstrate the influence of the grid refinement on the final design, the design domain is discretized with  $80 \times 40 = 3200$ ,  $120 \times 60 = 7200$  and  $160 \times 80 = 12800$  elements, respectively. The three numerical cases are performed with  $\Delta\tau = 10$  and  $\beta = 1e-6$ , and the related results are shown in Table 5. The numerical results in Table 5 show that consistent designs can be obtained with different level of grid refinements. In numerical implementation, the grid should be sufficiently fine to capture the spatial partial derivative of the scalar function crossing meshing grids, thus avoiding numerical artifacts contaminating the solution [7,18]. As far as explicit schemes are concerned, a fine spatial mesh indicates a large amount of iterations to fully advance the level set processing because of consideration of the CFL condition [60,2]. However, too much iteration will in turn degenerate the numerical stability due to the accumulation of truncation errors which is caused by the polynomial snaking phenomena. It was reported that the grid refinement scheme can enhance the possibility of finding a global minimum [6,25]. However, regarding the structural optimization problems, in general, it is difficult to obtain global solutions in most cases due to the nonconvexity of optimization problems [12], even if some mathematical programming methods [56] can ensure a series of strictly convex sub-optimization problems. The numerical results in Table 5 demonstrate that the present level set method can apply different meshes to produce consistent designs similar to widely accepted topology [12], but there is no guarantee that the present level set method can lead to a "global" optimum. In the present method, it can be seen that the length of time step size is not restricted by minimum spatial grid size, and the different grid levels can yield the similar final designs with the same step sizes. Thus, the present semi-implicit level set method is free from the CFL condition and also it is stable for all time step sizes.

## 7. Conclusion

In this paper, a semi-implicit level set method has been presented for structural shape and topology optimization. The semi-implicit AOS algorithm is being stable for all time steps and without strict restriction related to the satisfaction of the CFL condition. As a result, in solving the Hamilton–Jacobi PDE, the present method can obviously increase the computational efficiency of the topology optimization process, because the present semi-implicit scheme can totally relax the CFL condition relevant to the explicit time-marching schemes. With a natural extension of the velocity field, the shape sensitivity is evaluated in the entire design domain. Furthermore, in the standard level set method, the global reinitialization procedure has been utilized

as a time-consuming process to regularize the level set function periodically in the neighbor of the front, in order to retain a signed distance function to stabilize the numerical process. However, the proposed level set method has the capability of creating new holes inside the material domain via the boundary merging and splitting, leading to the final design being independent of the initial guess. This can be regarded as a main advantage of the present level set method over the standard level set methods. Therefore, as the numerical cases show, the method in this paper can avoid the unfavorable numerical features occurred in the standard level set method. The proposed level set method has reasonably included the advantages of the implicit level-set boundary representation and the semi-implicit AOS scheme. Furthermore, this method can be regarded as a general and a mathematically well-founded method for structural shape and topology optimization problems, and it can be easily and straightforwardly extended to more advanced optimization problems including complicated objective function and multiple constraints.

## Acknowledgments

This research was sponsored in part by the Australian Research Council (ARC-DP0666683), the Research Grants Council of Hong Kong (CUHK416205 and CUHK4164/03E), and the National “863” High-Tech Development Project of China (2006AA04Z162). The authors thank Prof. Stanly Osher and the anonymous reviewers for their valuable comments.

## References

- [1] G. Allaire, *Shape Optimization by the Homogenization Method*, Springer-Verlag, New York, 2001.
- [2] G. Allaire, F. Jouve, A.M. Toader, Structural optimization using sensitivity analysis and a level-set method, *Journal of Computational Physics* 194 (2004) 363–393.
- [3] G. Allaire, F. Jouve, A level-set method for vibration and multiple loads structural optimization, *Computer Methods in Applied Mechanics and Engineering* 194 (2005) 3269–3290.
- [4] G. Allaire, F. Jouve, Coupling the level set method and the topological gradient in structural optimization, in: M.P. Bendsøe, N. Olhoff, O. Sigmund (Eds.), *IUTAM Symposium on Topological Design Optimization of Structures, Machines and Materials*, vol. 137, 2006, pp. 3–12.
- [5] S. Amstutz, H. Andra, A new algorithm for topology optimization using a level-set method, *Journal of Computational Physics* 216 (2006) 573–588.
- [6] U.M. Ascher, E. Haber, Grid refinement and scaling for distributed parameter estimation problems, *Inverse Problem* 17 (2001) 571–590.
- [7] T. Belytschko, C. Parimi, N. Moes, N. Sukumar, S. Usui, Structured extended finite element methods for solids defined by implicit surfaces, *International Journal for Numerical Methods in Engineering* 56 (2002) 609–635.
- [8] T. Belytschko, S.P. Xiao, C. Parimi, Topology optimization with implicitly function and regularization, *International Journal for Numerical Methods in Engineering* 57 (2003) 1177–1196.
- [9] A.D. Belegundu, T.R. Chandrupatla, *Optimization Concepts and Applications in Engineering*, Prentice Hall, 1999.
- [10] M.P. Bendsøe, N. Kikuchi, Generating optimal topology in structural design using a homogenization method, *Computer Methods in Applied Mechanics and Engineering* 71 (2) (1988) 197–224.
- [11] M.P. Bendsøe, O. Sigmund, Material interpolation schemes in topology optimization, *Archive of Applied Mechanics* 69 (1999) 635–654.
- [12] M.P. Bendsøe, O. Sigmund, *Topology Optimization: Theory, Methods, and Applications*, Springer, Berlin Heidelberg, 2003.
- [13] M. Burger, B. Hacker, W. Ring, Incorporating topological derivatives into level set methods, *Journal of Computational Physics* 194 (2004) 344–362.
- [14] M. Burger, S.J. Osher, A survey on level set methods for inverse problems and optimal design, *European Journal of Applied Mathematics* 16 (2005) 263–301.
- [15] T. Cecil, J.L. Qian, S. Osher, Numerical methods for high dimensional Hamilton–Jacobi equations using radial basis functions, *Journal of Computational Physics* 196 (1) (2004) 327–347.
- [16] J.Q. Chen, V. Shapiro, K. Suresh, I. Tsukanov, Shape optimization with topological changes and parametric control, *International Journal for Numerical Methods in Engineering* 71 (2007) 313–346.
- [17] K.K. Choi, N.H. Kim, *Structural Sensitivity Analysis and Optimization I-Linear Systems*, Springer, New York, 2005.
- [18] K. Doel, U.M. Ascher, On level set regularization for highly ill-posed distributed parameter estimation problems, *Journal of Computational Physics* 216 (2006) 707–723.
- [19] D. Enright, F. Losasso, R.P. Fedkiw, A fast and accurate semi-Lagrangian particle level set method, *Computers and Structures* 83 (2005) 479–490.
- [20] D. Enright, R. Fedkiw, J. Ferziger, I. Mitchell, A hybrid particle level set method for improved interface capturing, *Journal of Computational Physics* 183 (2002) 83–116.

- [21] H. Eschenauer, V. Kobelev, A. Schumacher, Bubble method for topology and shape optimization of structures, *Structural and Multidisciplinary Optimization* 8 (1994) 142–151.
- [22] H. Eschenauer, N. Olhoff, Topology optimization of continuum structures: a review, *Applied Mechanics Review* 54 (2001) 331–390.
- [23] F. Gournay, Velocity extension for the level-set method and multiple eigenvalues in shape optimization, *SIAM Journal on Control and Optimization* 45 (2006) 343–367.
- [24] E. Haber, A multilevel level-set method for optimizing eigenvalues in shape design problems, *Journal of Computational Physics* 198 (2004) 518–534.
- [25] E. Haber, J. Modersitzki, A multilevel method for image registration, *SIAM Journal of Scientific Computing* 27 (5) (2006) 1594–1607.
- [26] D.S. Harned, D.D. Schnack, Semi-implicit method for long time scale magnetohydrodynamic computations in three dimensions, *Journal of Computational Physics* 65 (1986) 57–70.
- [27] B. Hassani, E. Hinton, A review of homogenization and topology optimization III-topology optimization using optimality criteria, *Computers and Structures* 69 (1998) 739–756.
- [28] L. He, C.Y. Kao, S. Osher, Incorporating topological derivatives into shape derivative based level set methods, *Journal of Computational Physics* 225 (2007) 891–909.
- [29] E.J. Hwang, K.K. Chioi, V. Kov, *Design Sensitivity Analysis of Structural Systems*, Academic Press, Orlando, 1986.
- [30] H.W. Li, X.C. Tai, Piecewise constant level set methods for multiphase motion, *International Journal of Numerical Analysis and Modeling* 4 (2007) 274–293.
- [31] T. Lu, T. Neittaanmaki, X.C. Tai, A parallel splitting up method and its application to Navier–Stokes equations, *Applied Mathematics Letters* 4 (1991) 25–29.
- [32] Z. Luo, M.Y. Wang, S.Y. Wang, P. Wei, A level set-based parameterization method for structural shape and topology optimization, *International Journal for Numerical Methods in Engineering* (2007), doi:10.1002/nme.2092.
- [33] Z. Luo, L.Y. Tong, M.Y. Wang, S.Y. Wang, Shape and topology optimization of compliant mechanisms using a parameterization level set method, *Journal of Computational Physics* 227 (2007) 680–705.
- [34] G.S. Jiang, D. Peng, Weighted ENO schemes for Hamilton–Jacobi equations, *SIAM Journal on Scientific Computing* 21 (2000) 2126–2143.
- [35] I.M. Mitchell, A toolbox of level set methods, Technical Report, TR-2004-09, Department of Computer Science, University of British Columbia, Canada, 2004.
- [36] F. Murat, S. Simon, *Etudes de problèmes d’optimal design*, Lecture Notes in Computer Science, vol. 41, Springer-Verlag, Berlin, 1976, pp. 54–62.
- [37] J. Nocedal, S.J. Wright, *Numerical Optimization*, Springer, New York, 1999.
- [38] J. Norato, J.R. Haber, D. Tortorelli, M.P. Bendsøe, A Geometry Projection Method for Shape Optimization, *International Journal for Numerical Methods in Engineering* 60 (2004) 2289–2312.
- [39] A.A. Novotny, R.A. Feijoo, E. Taroco, C. Padra, Topological-shape sensitivity analysis, *Computer Methods in Applied Mechanics and Engineering* 192 (2003) 803–829.
- [40] S. Osher, J.A. Sethian, Front propagating with curvature dependent speed: algorithms based on Hamilton–Jacobi formulations, *Journal of Computational Physics* 78 (1988) 12–49.
- [41] S. Osher, R.P. Fedkiw, Level set methods: an overview and some recent results, *Journal of Computational Physics* 169 (2) (2001) 463–502.
- [42] S. Osher, F. Santosa, Level-set methods for optimization problem involving geometry and constraints: I. Frequencies of a two-density inhomogeneous drum, *Journal of Computational Physics* 171 (2001) 272–288.
- [43] S. Osher, R.P. Fedkiw, *Level Set Methods and Dynamic Implicit Surface*, Springer-Verlag, New York, 2002.
- [44] S. Osher, N. Paragios, *Geometric Level Set Methods in Imaging, Vision, and Graphics*, Springer-Verlag, New York, 2003.
- [45] G.I.N. Rozvany, U. Kirsch, M.P. Bendsøe, O. Sigmund, Layout optimization of structures, *Applied Mechanics Reviews* 48 (1995) 41–119.
- [46] G.I.N. Rozvany, Aim, scope, methods, history and unified terminology of computer-aided topology optimization in structural mechanisms, *Structural and Multidisciplinary Optimization* 21 (2001) 90–108.
- [47] D. Peng, B. Merriman, S. Osher, H. Zhao, M. Kang, A PDE-based fast local level set method, *Journal of Computational Physics* 155 (1999) 410–438.
- [48] J.A. Sethian, *Level set methods and fast marching methods: evolving interfaces in computational geometry, fluid mechanics, computer vision and material science*, Cambridge Monograph on Applied and Computational Mathematics, Cambridge University Press, UK, 1999.
- [49] J.A. Sethian, A. Wiegmann, Structural boundary design via level set and immersed interface methods, *Journal of Computational Physics* 163 (2000) 489–528.
- [50] M. Sussman, E. Fatemi, An efficient interface-preserving level set re-distancing algorithm and its application to interfacial incompressible fluid flow, *SIAM Journal on Scientific Computing* 20 (1999) 1165–1191.
- [51] O. Sigmund, J. Petersson, Numerical instabilities in topology optimization: a survey on procedures dealing with checkerboards, mesh-dependencies and local minima, *Structural and Multidisciplinary Optimization* 16 (1998) 68–75.
- [52] O. Sigmund, A 99 line topology optimization code written in MATLAB, *Structural and Multidisciplinary Optimization* 31 (2001) 419–429.
- [53] O. Sigmund, Design of multiphysics actuator using topology optimization – Part I: one material structure, *Computer Methods in Applied Mechanics and Engineering* 190 (2001) 6577–6604.
- [54] J. Sokolowski, J.P. Zolesio, *Introduction to Shape Optimization: Shape Sensitivity Analysis*, Springer, Berlin, 1992.

- [55] J. Sokolowski, A. Zochowski, On the topological derivative in shape optimization, *SIAM Journal of Control Optimization* 37 (1999) 1251–1272.
- [56] K. Svanberg, The method of moving asymptotes: a new method for structural optimization, *International Journal for Numerical Methods in Engineering* 24 (1987) 359–373.
- [57] X.C. Tai, O. Christiansen, P. Lin, I. Skjaelaaen, Image segmentation using some piecewise constant level set methods with MBO type of project, *International Journal of Computer Vision* 73 (2007) 61–76.
- [58] R. Tsai, S. Osher, Level set methods and their applications in image science, *Communications in Mathematical Sciences* 1 (4) (2003) 623–656.
- [59] W.Y. Tang, L.Y. Tong, Y.X. Gu, Improved genetic algorithm for design optimization of truss structures with size, shape and topology variables, *International Journal for Numerical Methods in Engineering* 62 (2005) 1737–1762.
- [60] M.Y. Wang, X.M. Wang, D.M. Guo, A level set method for structural topology optimization, *Computer Methods in Applied Mechanics and Engineering* 192 (2003) 217–224.
- [61] M.Y. Wang, X.M. Wang, ‘Color’ level sets: a multiphase method for structural topology optimization with multiple materials, *Computer Methods in Applied Mechanics and Engineering* 193 (2004) 469–496.
- [62] M.Y. Wang, P. Wei, Topology optimization with level set method incorporating topological derivatives, in: *Proceedings of 6th World Congress of Structural and Multidisciplinary Optimization (WCSMO6)*, May 2005, Rio de Janeiro, Brazil.
- [63] S.Y. Wang, M.Y. Wang, Radial basis functions and level set method for structural topology optimization, *International Journal for Numerical Methods in Engineering* 65 (2006) 2060–2090.
- [64] S.Y. Wang, M.Y. Wang, Structural shape and topology optimization using an implicit free boundary parameterization method, *Computer Modeling in Engineering and Science* 13 (2006) 119–147.
- [65] S.Y. Wang, K.M. Lim, B.C. Khoo, M.Y. Wang, An extended level set method for shape and topology optimization, *Journal of Computational Physics* 221 (2007) 395–421.
- [66] P. Wei, M.Y. Wang, A piecewise constant level set method for structural shape and topology optimization, in: *Seventh World Congress of Structural and Multidisciplinary Optimization*, Seoul, Korea, 2007.
- [67] J. Weickert, B.M. Romeny, M. Viergever, Efficient and reliable schemes for nonlinear diffusion filtering, *IEEE Transaction on Image Processing* 7 (1998) 398–410.
- [68] J. Weickert, Applications of nonlinear diffusion in image processing and computer vision, Technical Report 18/2000, University of Mannheim, 68131 Mannheim, Germany, 2000.
- [69] J. Weickert, Efficient image segmentation using partial differential equations and morphology, *Pattern Recognition* 34 (2001) 1813–1824.
- [70] Y.M. Xie, G.P. Steven, A simple evolutionary procedure for structural optimization, *Computers and Structures* 49 (1993) 885–896.
- [71] M. Zhou, G.I.N. Rozvany, The COC algorithm, Part II: topological, geometry and generalized shape optimization, *Computer Methods in Applied Mechanics and Engineering* 89 (1991) 197–224.